

The ceramide moiety of disialoganglioside (GD3) is essential for GD3 recognition by the sialic acid-binding lectin SIGLEC7 on the cell surface

Received for publication, December 12, 2018, and in revised form, May 18, 2019. Published, Papers in Press, May 28, 2019, DOI 10.1074/jbc.RA118.007083

Noboru Hashimoto^{‡§}, Shizuka Ito[‡], Akiko Tsuchida[‡], Robiul H. Bhuiyan^{‡¶}, Tetsuya Okajima[‡], Akihito Yamamoto[§], Keiko Furukawa[¶], Yuhsuke Ohmi[¶], and Koichi Furukawa^{‡¶1}

From the [‡]Department of Biochemistry II, Nagoya University Graduate School of Medicine, 65 Tsurumai, Showa-ku, Nagoya 466-0065, Japan, the [¶]Department of Biomedical Sciences, Chubu University College of Life and Health Sciences, 1200 Matsumoto, Kasugai, Aichi 487-8501, Japan, and the [§]Department of Tissue Regeneration, Tokushima University Graduate School of Biomedical Sciences, 3-18-5, Kuramoto-cho, Tokushima 770-8504, Japan

Edited by Gerald W. Hart

To analyze the binding specificity of a sialic acid-recognizing lectin, sialic acid-binding Ig-like lectin 7 (SIGLEC7), to disialyl gangliosides (GD3s), here we established GD3-expressing cells by introducing GD3 synthase (*GD3S* or *ST8SIA1*) cDNA into a colon cancer cell line, DLD-1, that expresses no ligands for the recombinant protein SIGLEC7-Fc. SIGLEC7-Fc did not recognize newly-expressed GD3 on DLD-1 cells, even though GD3 was highly expressed, as detected by an anti-GD3 antibody. Because milk-derived GD3 could be recognized by this fusion protein when incorporated onto the surface of DLD-1 cells, we compared the ceramides in DLD-1-generated and milk-derived GD3s to identify the SIGLEC7-specific GD3 structures on the cell membrane, revealing that SIGLEC7 recognizes only GD3-containing regular ceramides but not phytoceramides. This was confirmed by knockdown/knockout of the sphingolipid delta(4)-desaturase/C4-monooxygenase (*DES2*) gene, involved in phytoceramide synthesis, disclosing that *DES2* inhibition confers SIGLEC7 binding. Furthermore, knocking out fatty acid 2-hydroxylase also resulted in the emergence of SIGLEC7 binding to the cell surface. To analyze the effects of binding between SIGLEC7 and various GD3 species on natural killer function, we investigated cytotoxicity of peripheral blood mononuclear cells from healthy donors toward GD3S-transfected DLD-1 (DLD-1-GD3S) cells and DLD-1-GD3S cells with modified ceramides. We found that cytotoxicity is suppressed in DLD-1-GD3S cells with dehydroxylated GD3s. These results indicate that the ceramide structures in glycosphingolipids affect SIGLEC7 binding and distribution on the cell surface and influence cell sensitivity to killing by SIGLEC7-expressing effector cells.

There have been a number of studies on cancer-associated carbohydrate antigens (1). Some of them are utilized as tumor markers (2). In addition to roles as tumor markers, the function of sialic acid-containing glycosphingolipids, gangliosides have been rigorously analyzed (3). In particular, the roles of disialyl gangliosides in cancer phenotypes have been reported by us (4, 5) and many other groups (6, 7). Among them, GD3² and GD2 are representative cancer-associated gangliosides, and the mechanisms for their actions have been reported recently. Melanoma-associated ganglioside GD3 enhances malignant properties of melanomas (3) and gliomas (8) by physically associating with membrane function molecules such as neogenin (9) and platelet-derived growth factor receptor α (8), respectively. These interactions between disialyl gangliosides and membrane molecules are exerted by *cis*-reaction on the same membrane.

There are a number of *trans*-acting ligands for glycosphingolipids, such as bacterial toxins (10) and sialic acid-binding lectins, Siglecs (11). The recognized structures of sialyl compounds by Siglecs have been available based on the results of binding assay using a sugar array fixed on plates or membranes (12) (<http://www.functionalglycomics.org>).³ From these results, Siglec-7 has been considered to react mainly with disialyl structures such as disialyl Lewis a (13), disialyl galactosyl globoside (14), and ganglioside GD3 (15), although it seems hard to find common structures among them.

To analyze binding specificity of Siglec-7 toward disialyl gangliosides, we have established GD3-expressing transfectant cells by introducing GD3 synthase (*GD3S*) (*ST8SIA1*) cDNA into a colon cancer cell line, DLD-1, that expresses no ligands

This work was supported by Grants-in-aid from the Ministry of Education, Culture, Sports and Technology of Japan (MEXT) 15H04696, 15K15080, 25670141, and 24390078, Grant-in-aid for Young Scientists (B) 26860320, and by a grant from Yokoyama Rinsho Yakuri Foundation. The authors declare that they have no conflicts of interest with the contents of this article.

This article contains Figs. S1–S6.

¹ To whom correspondence should be addressed: Dept. of Biomedical Sciences, Chubu University College of Life and Health Sciences, 1200 Matsumoto, Kasugai, Aichi, 487-8501, Japan. Tel.: 81-568-51-9512; Fax: 81-568-51-9512; E-mail: koichi@isc.chubu.ac.jp.

² The abbreviations used are: GD3, Sia α 2,8Sia α 2,3Gal β 1,4Glc-Cer; GD2, Sia α 2,8Sia α 2,3 (GalNAc β 1,4) Gal β 1,4 Glc-Cer; Siglec, sialic acid-binding immunoglobulin-like lectin; *ST8SIA1*, GD3 synthase; *DES2*, dihydroceramide 4-desaturase; C-4 hydroxylase; FA2H, fatty acid 2-hydroxylase; FCM, flow cytometry; PBMC, peripheral blood mononuclear cell; sgRNA, single-guide RNA; DMEM, Dulbecco's modified Eagle's medium; TfR, transferrin receptor; PFA, paraformaldehyde; TDE, 2,2'-thiodirithanol; SR-SIM, super-resolution structured illumination microscopy; FA, fatty acid; LCB, long-chain base; C, chloroform; M, methanol; MRM, multiple reaction monitoring; EGFP, enhanced GFP; HILIC, hydrophilic interaction liquid chromatography; HPTLC, high performance TLC.

³ Please note that the JBC is not responsible for the long-term archiving and maintenance of this site or any other third party hosted site.

Ceramide structures involved in the recognition of Siglec-7

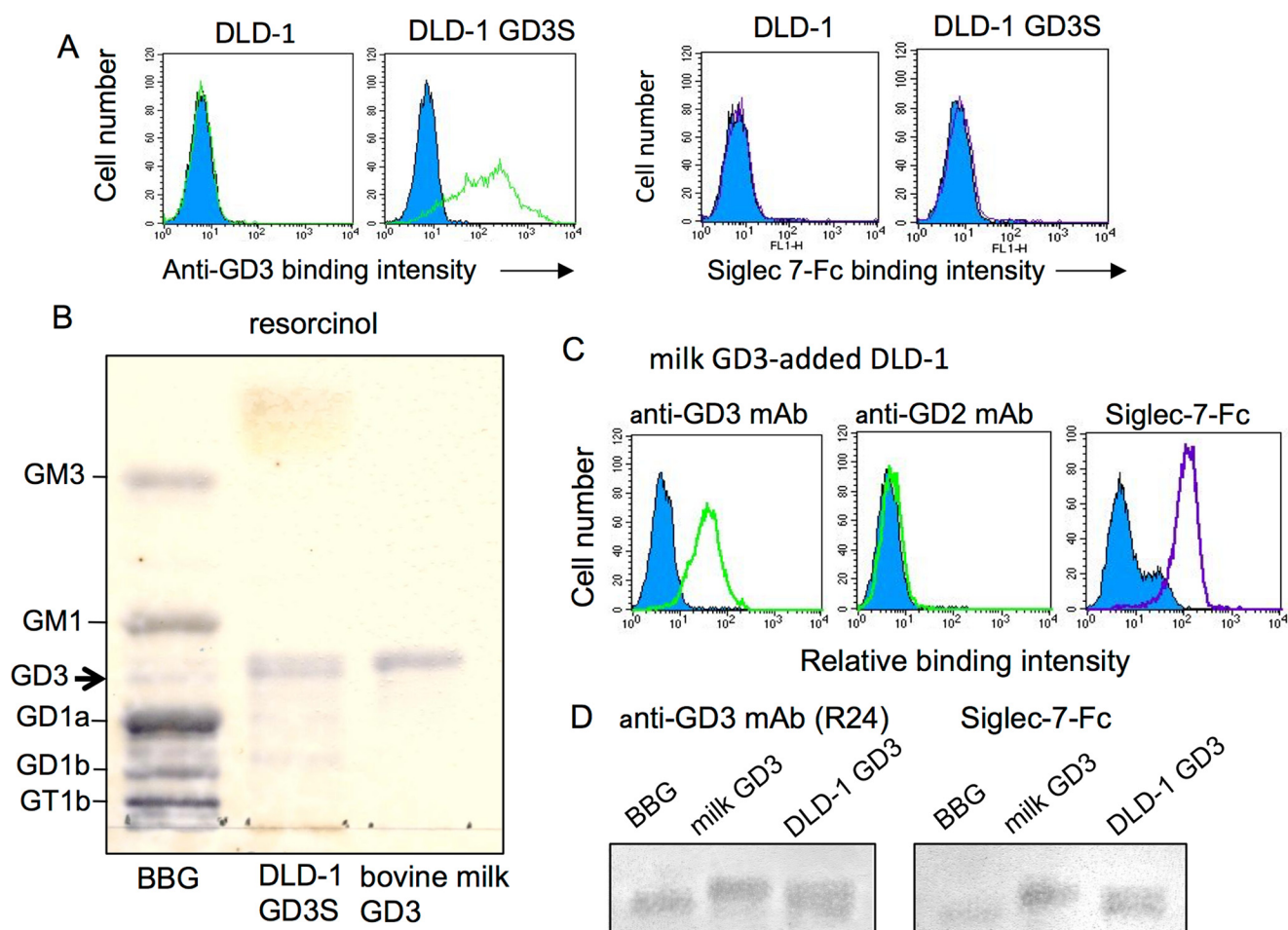


Figure 1. Differential binding of Siglec-7-Fc to GD3. *A*, flow cytometry analysis. *Green lines* indicate expression levels of GD3 on parent DLD-1 and GD3 synthase cDNA-transfected DLD-1 GD3S as analyzed by anti-GD3 mAb (R24). *Purple lines* indicate Siglec-7-Fc-binding levels. *B*, acidic glycolipids were isolated from DLD-1 GD3S using DEAE-Sephadex A-50TM. Resorcinol spray was performed to detect sialic acids on gangliosides. *BBG*, bovine brain gangliosides as a control. *C*, bovine milk-derived GD3 was added to DLD-1 culture medium at 12.5 mM. After 5 h, cells were analyzed with FCM for ganglioside expression (anti-GD3 and anti-GD2 mAbs) and Siglec-7-Fc binding. *D*, TLC-immunostaining was performed with mAb R24 or Siglec-7-Fc.

for Siglec-7-Fc. During binding analysis of Siglec-7 with these transfectant cells, we found that newly expressed GD3 on DLD-1 cells was not recognized by Siglec-7-Fc, whereas milk-derived GD3 could be recognized when incorporated onto the cell surface of DLD-1. Therefore, fine-structure specificity of GD3 recognized by Siglec-7 on the cell membrane has been studied. Consequently, involvement of ceramide portions in the binding of Siglec-7 to GD3 has been elucidated.

Results

A sialic acid-recognizing lectin, Siglec-7, is expressed as an inhibitory receptor on the cell surface of NK cells and a part of monocytes (12). To examine reactivity of Siglec-7 to sialylated glycolipids, we focused on the binding of Siglec-7-Fc to a representative disialyl ganglioside (GD3) (15) expressed on the cell surface. Molecular form and purity of Siglec-7-Fc are shown in Fig. S1. To facilitate evaluation of binding of Siglec-7 to sialylated sugar chains and purification of secreted proteins, Siglec-7-Fc was used in this study.

To observe specific interaction of GD3 and Siglec-7 on the cell surface, we introduced cDNA of GD3S (*ST8SIA1*) into a colon cancer cell line, DLD-1, that did not express GD3. It was

also negative for Siglec-7-Fc binding. This condition enabled us to selectively observe the roles of GD3 as a Siglec-7 ligand. Established GD3+ DLD-1 (DLD-1 GD3S) expressed a high level of GD3 as detected by flow cytometry (FCM) using anti-GD3 monoclonal antibody (mAb) R24 (Fig. 1*A*, left panel). When reactivity of Siglec-7-Fc with this transfectant cell was examined, no binding of Siglec-7-Fc could be detected (Fig. 1*A*, right panel).

Then, gangliosides were extracted from DLD-1 GD3S cells and analyzed by HPTLC and subsequent resorcinol spray. As expected, GD3 bands were detected in the acidic fraction of extracts from DLD-1 GD3S (Fig. 1*B*). To analyze reactivity of Siglec-7 with GD3 from other sources, milk-derived GD3 was added to the culture medium of DLD-1, leading to incorporation of exogenous GD3 and re-expression on the cell surface. Milk-derived GD3 was expressed on DLD-1 as detected by FCM using mAb R24 (Fig. 1*C*, left panel). GD2, a derivative of GD3, was not expressed on DLD-1 as analyzed using anti-GD2 mAb (Fig. 1*C*, middle panel). Siglec-7-Fc also bound to GD3 on the cell surface of milk GD3-incorporated DLD-1 (Fig. 1*C*, right panel), indicating that Siglec-7 discriminated some structural differences in GD3 between those generated in

DLD-1 and those incorporated onto DLD-1 from milk-derived gangliosides.

The thin-layer chromatography (TLC) immunostaining of these extracts with anti-GD3 mAb or Siglec-7-Fc revealed that both DLD-1 GD3S-generated GD3 and milk-derived GD3 were detected by the mAb and also by Siglec-7-Fc as shown in Fig. 1D.

To clarify structural differences in GD3 from DLD-1 GD3S and milk-derived gangliosides, mass spectrometry (MS) analysis was performed using a triple quadrupole mass spectrometer with a precursor ion scan with the product ion of sialic acid ($[\text{Neu5Ac-H}]^-$, m/z 290). GD3 formed mainly $[\text{M} - 2\text{H}]^{2-}$ ions (Fig. S2). As shown in Fig. 2, MS analysis revealed abundant GD3 d18:1-23:0 (m/z 770) in the milk-derived sample, and GD3 t18:0-24:1/d18:1-24:0h (m/z 785) in DLD-1 GD3S-derived samples. Although milk-derived GD3 contained only regular (d18:1/d16:1) forms of ceramide (Fig. 2A, upper panel), DLD-1 GD3S-generated GD3 mainly consisted of aberrant peaks with +8 m/z units or +16 Da (molecular mass) compared with regular forms of GD3 as major components (Fig. 2A, lower panel), suggesting the presence of additional hydroxylation in the ceramide portion.

DES1 enzyme synthesizes ceramide via dihydroceramide in the *de novo* synthesis. As main modes for modification of ceramide structures with a focus on hydroxylation, C4 hydroxylation of long-chain bases (LCBs) and C2 hydroxylation of fatty acids can be raised (Fig. 2B). The former is catalyzed by DES2 enzyme along with saturation of unsaturated bond between C4 and C5, resulting in the formation of phytoceramide. The latter is catalyzed by fatty acid C2 hydroxylase (FA2H) (Fig. 2B). Representative products from these reactions are shown in Fig. 2C.

Here, we performed MS/MS analysis of individual GD3 in negative and positive ion mode (Fig. 3). Common peaks between two samples (negative mode m/z 777 and positive mode m/z 779 in milk versus m/z 777 and 779 in DLD-1 GD3S) showed identical MS/MS fragmentation. There were no differences in sugar portions, but definite differences were detected in ceramides between the most abundant GD3 species of them (negative ion mode m/z 770 and positive ion mode m/z 772 in milk versus negative ion mode m/z 785 and positive ion mode m/z 787 in DLD-1 GD3S) (Fig. 3, A, B, G, and H). In MS/MS analysis of ceramide, hydroxylated acyl ion (FA C24:0 h, m/z 408 $[\text{M} - \text{H}]^-$) (left panel) and unsaturated acyl ion (FA C24:1, m/z 366 $[\text{M} + \text{H}]^+$) (right panel) were characteristically detected in GD3 (t18:0-24:1/d18:1-24:0 h, m/z 785 $[\text{M} - 2\text{H}]^{2-}$ and m/z 787 $[\text{M} + 2\text{H}]^{2+}$) from DLD-1 GD3S, whereas hydroxylated fragments of LCB were hard to detect because only the mass of dehydrated ion was generated from phytoceramide. However, GD3 should have phytoceramide when calculated as the fatty acid is C24:1. Consequently, milk-derived GD3 consisted of regular forms of ceramide with saturated FA (Figs. 2A, upper panel, and 3, upper panel), and the majority of DLD-1 GD3S-derived GD3 contained phytoceramide or 2-OH FA (Figs. 2A, lower panel, and 3, lower panel).

Furthermore, structures of ganglioside GM3 was compared between bovine milk-derived samples and extracts from three colon cancer cell lines, DLD-1, Caco-2, and WiDr, as well as DLD-1 GD3S. All these cell lines expressed GM3 as a major

ganglioside. WiDr expressed high levels of DES2 and FA2H. Caco-2 also expressed these two genes at high levels as WiDr cells (Fig. S3). As shown in Fig. 4A, bovine milk GM3 had regular type LCB and saturated FA, whereas major peaks of DLD-1-derived GM3 were hydroxylated either in LCB or FA as shown in GD3. Ganglioside profiles from Caco-2 and WiDr also showed that major peaks were of hydroxylated LCB and/or FA. GM3 with regular ceramide form was minor (Fig. 4B). TLC/resorcinol revealed that GM3 from these colon cancer cell lines contained multiple components more slowly migrating than that of bovine brain tissues (Fig. 4C).

Thus, it was suggested that DLD-1 GD3S-generated GD3 mainly contained hydroxylated ceramides (phytoceramide or 2-OH ceramide). In the biosynthetic pathway of ceramide, dihydroceramide is converted to ceramide by forming unsaturated bonds between C4 and C5 of LCB with sphingolipid Δ 4-desaturase (DES1). In contrast, DES2 (a family of DES1) synthesizes phytoceramide by C4 hydroxylation in LCB as shown in Fig. 2B. Then, we established the DLD-1 GD3S line with the knockout of the *DES2* gene using CRISPR/Cas9 system. Genome sequences of the gene in the DLD-1 GD3S with *DES2* KO are shown in Fig. 5A. Deletion in two alleles (deletion of 52 nucleotides and insertion of a nucleotide and deletion of 31 nucleotides) in the *DES2* gene is demonstrated in Fig. 5A, top panel. Complete knockout of the *DES2* gene (and *FA2H*) was also confirmed by PCR with confronting two-pair primers system (Fig. S5), because current immunoblotting or RT-PCR seemed not so efficient to demonstrate minimal changes in the gene products, proteins, and mRNAs. Different migration from that of the original DLD-1 GD3S line was shown in Fig. 5B. In MRM analysis, the ratio (%) of GD3 containing hydroxylated ceramide was largely reduced (Fig. 5C and Fig. S4), whereas some GD3 species still remain to be more hydroxylated than the regular form.

In the binding of Siglec-7-Fc, DLD-1 GD3S with *DES2* KO showed definite binding of Siglec-7 (Fig. 5D, upper panel), whereas GD3 expression levels as detected by anti-GD3 mAb were persistently positive (Fig. 5D, lower panel).

As enzymes to catalyze hydroxylation of ceramides, FA2H has been also known. Fatty acids undergoing hydroxylation by FA2H are transferred to sphingosine by ceramide synthases, leading to the synthesis of 2-OH ceramide or 2-OH phytoceramide. Then, we also established *FA2H* KO cells using DLD-1 GD3S cells. Deleted genome sequences of the gene are shown in Fig. 5A. Deletion of one nucleotide and four nucleotides in the individual alleles was demonstrated. KO of *FA2H* was also performed in DLD-1 GD3S *DES2* KO cells with the CRISPR/Cas9 system as shown in Fig. 5A, bottom panel. DLD-1 GD3S cells deleted of *FA2H* also showed positive binding of Siglec-7-Fc (Fig. 5D, left lower panel). Double KO of two genes (*DES2* and *FA2H*) in DLD-1 GD3S cells showed further increased binding of Siglec-7-Fc (Fig. 5, D and E). Mean fluorescence intensities of Siglec-7-Fc binding as shown in Fig. 5D were presented in Fig. 5E.

Localization and distribution of GD3 generated in the cells or incorporated from exogenous gangliosides-containing medium were compared by immunocytochemistry as shown in Fig. 6A. In DLD-1 GD3S, GD3 was stained mainly on the cell

Ceramide structures involved in the recognition of Siglec-7

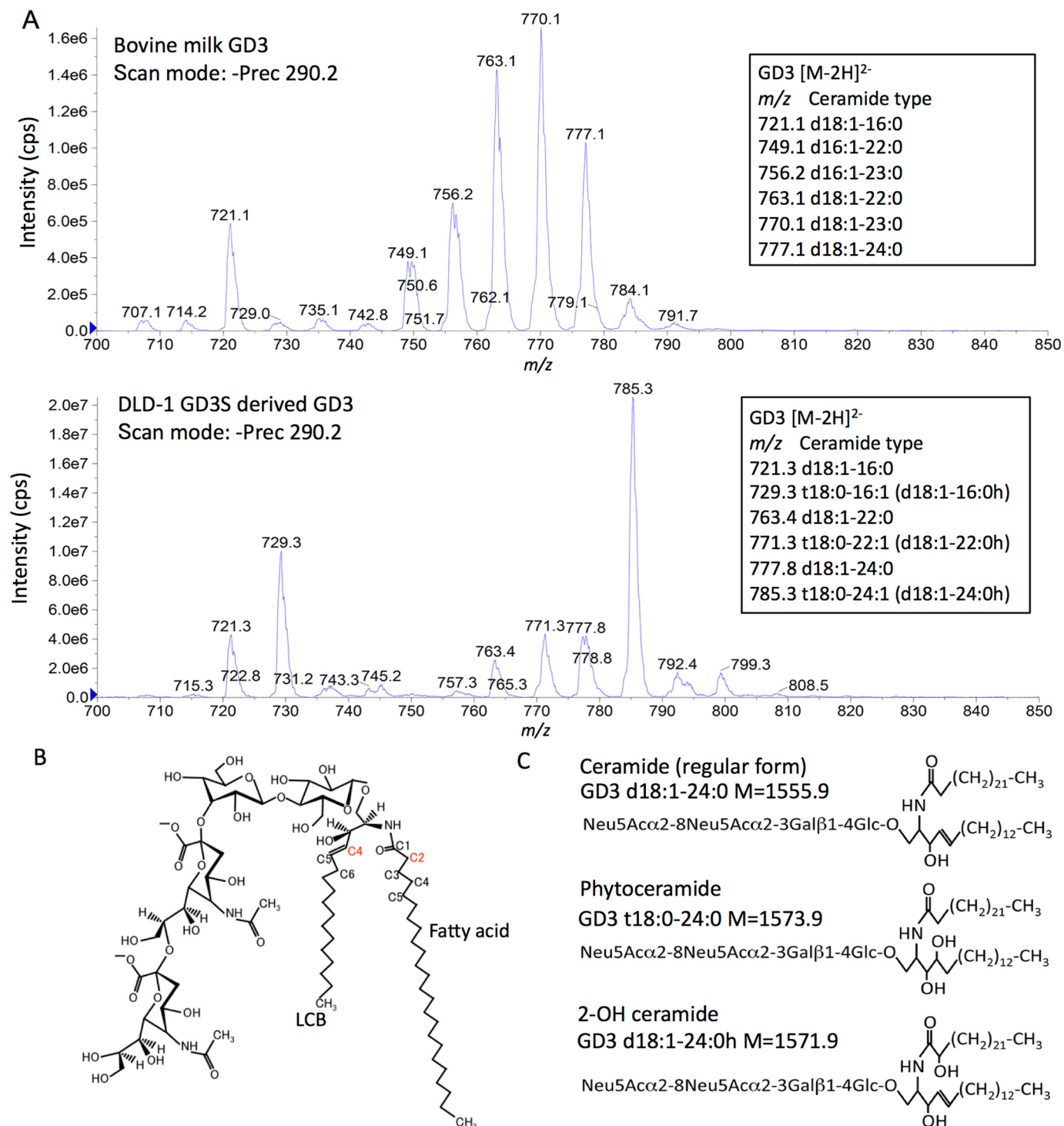


Figure 2. Structure analysis of bovine milk- and DLD-1 GD3S-derived ganglioside GD3. A, identification of ganglioside GD3 structure by MS. Precursor ion scan of m/z 290 (the sialic acid-derived product ion in a negative ion mode) shows several molecular species of ganglioside GD3. *Upper panel*, mass spectrum of bovine milk-derived GD3. *Lower panel*, DLD-1 GD3S-derived GD3. Carbon numbers of LCB were identified by MS/MS analysis (data not shown). B, long chain base C4 (red) is hydroxylated by DES2 (phytoceramide). Fatty acid C2 (red) is hydroxylated by FA2H (2-OH ceramide). C, structures of ceramide (regular form), phytoceramide, and 2-OH ceramide of GD3 are presented.

membrane with a relatively diffuse pattern (Fig. 6A, upper panel). In contrast, milk-derived GD3 incorporated into DLD-1 was also detected mainly on the membrane but with a speckled pattern (Fig. 6A, lower panel).

To analyze biological effects of binding between Siglec-7 and various forms of GD3 on NK function, cytotoxic activity of

PBMCs from healthy donors toward DLD-1 GD3S cells and DLD-1 GD3S cells with KO of *DES2* and/or *FA2H* was measured. Consequently, significant suppression of cytotoxic activity was observed in DLD-1 GD3S cells with KO of *DES2* and/or *FA2H* that were positive for Siglec-7-Fc binding compared with the original DLD-1 GD3S cells (Fig. 6B).

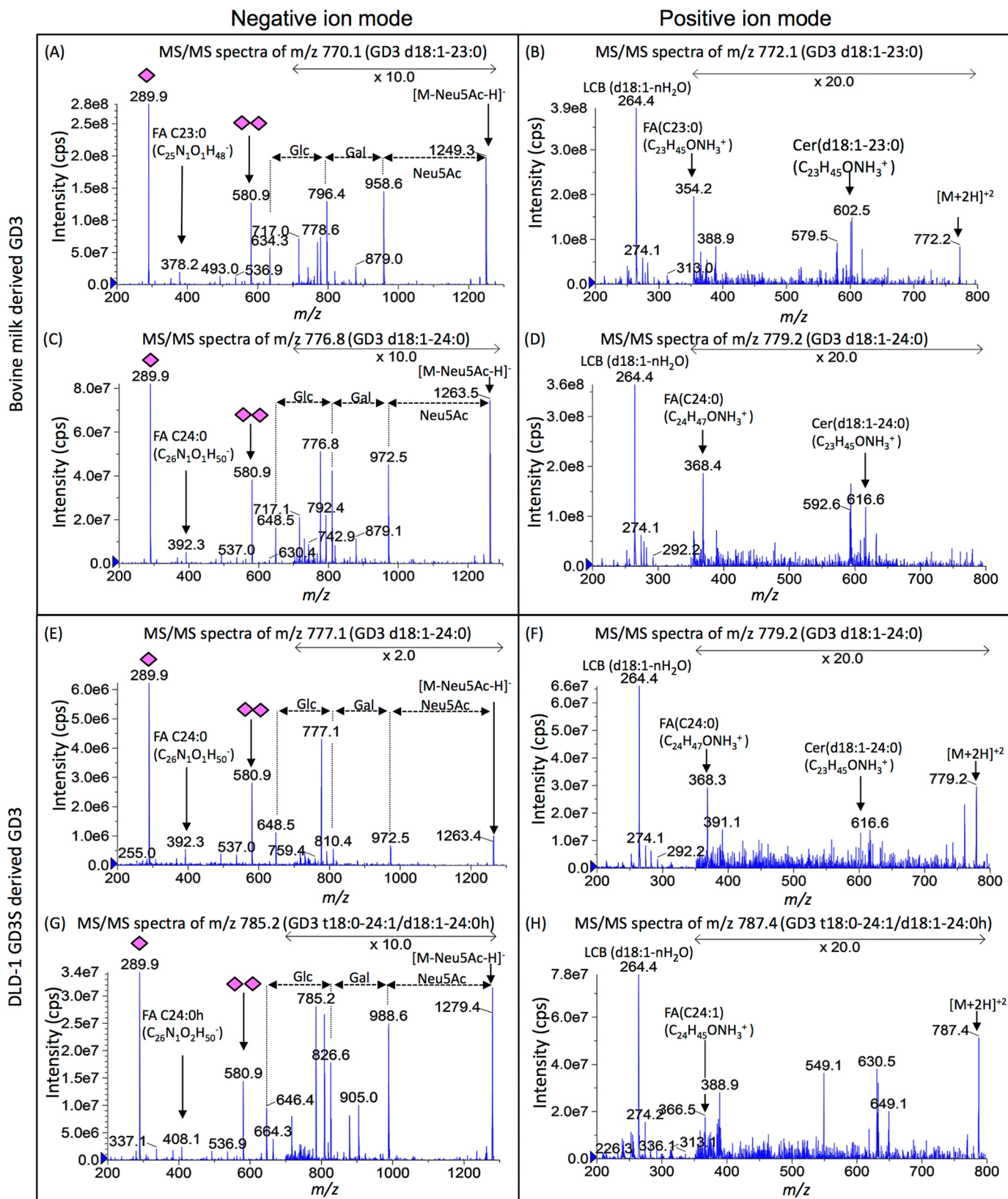


Figure 3. MS/MS fragmentation for major components of bovine milk- and DLD-1 GD3S-derived GD3. To clarify differences in their GD3 structures, a major peak and a common peak were chosen. The m/z 770 and 777 in bovine milk-derived GD3 and m/z 785 and 777 in DLD-1 GD3S-derived GD3 with precursor ion scan of negative ion mode were analyzed by enhanced product ion scan (MS/MS) of negative and positive ion mode. The *left column* is negative ion mode for analysis of glycan and fatty acid. The *right column* is positive ion mode for analysis of long chain base and fatty acid. As shown in negative ion mode, there was no difference in their glycan structures (A, C, E, and G). FA C23:0 (m/z 378 and 354) were detected in A and B. FA C24:0 (m/z 392 and 368) was detected in C and D and E and F. FA C24:0h (m/z 408) was detected in G. FA C24:1 (m/z 366) was detected in G. Therefore, m/z 770 in milk GD3 was identified as GD3 d18:1-23:0 (A and B). m/z 777 in milk GD3 and DLD-1 GD3S were identified as GD3 d18:1-24:0 (C-F). m/z 785 in DLD-1 GD3S was identified as GD3 t18:0-24:1/d18:1-24:0h (G and H).

Ceramide structures involved in the recognition of Siglec-7

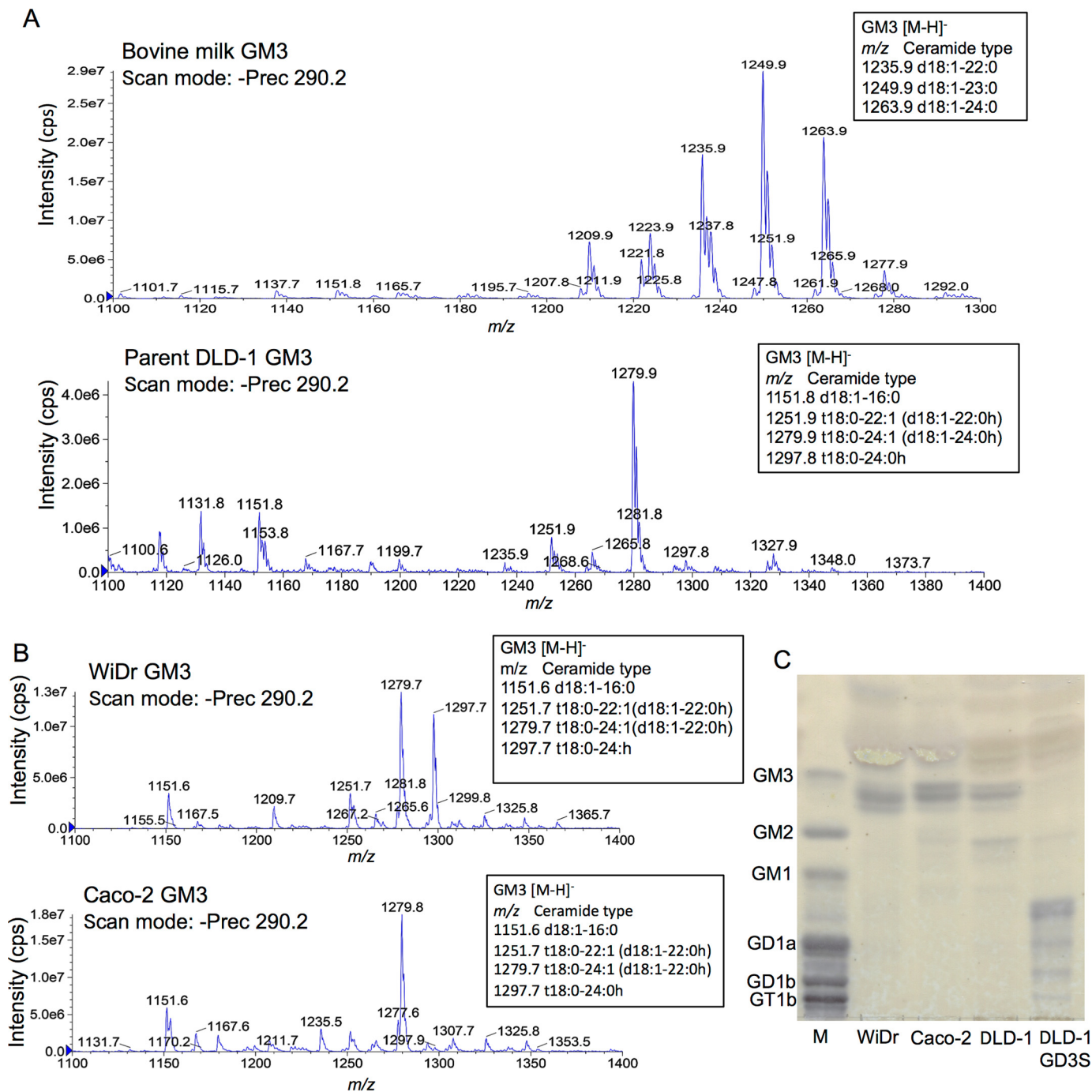


Figure 4. Analysis of bovine milk- and colon cancer cell-derived ganglioside GM3. A, as shown in the case of GD3, monosialyl ganglioside GM3 was analyzed. Bovine milk GM3 had saturated ceramide moiety and major peaks of DLD-1-derived GM3 were hydroxylated as GD3. B and C, ganglioside profiles of colon cancer cell lines. Gangliosides were isolated from colon cancer cell lines WiDr and Caco-2 and analyzed by MS (B), and also by TLC-resorcinol with those of DLD-1 and DLD-1 GD3S (C). M, bovine brain ganglioside mixture.

From these results, it was demonstrated that chemical structures of ceramides in glycosphingolipid molecules crucially affect the binding of Siglec-7 and also sensitivity to the killing by Siglec-7-expressing effector cells, NK cells.

To further analyze intracellular localization of GD3 in these DLD-1-transfectant cells, gangliosides were extracted from raft and nonraft fractions of DLD-1 GD3S cells and those with DES2-knockdown or those with FA2H-KO cells and served for TLC immunostaining. As shown in Fig. 7, B and C, DES2 knockdown or FA2H KO resulted in a shift of GD3 to lipid rafts,

whereas DLD-1 GD3S contained GD3 much more in nonraft fractions. Immunocytostaining of GD3 by anti-GD3 mAb R24 also (Fig. S6) revealed contrasting distribution patterns of GD3 between DLD-1 GD3S and other dehydroxylated sublines, *i.e.* DLD-1 GD3S DES2 KO, FA2H KO, and double KO (DKO) cells as shown in Fig. S6, A and B.

Finally, intracellular localization of GD3 was analyzed using a super-resolution microscope as shown in Fig. 8. Although DLD-1 GD3 showed white color indicating co-localization of GD3 (*magenta*, Alexa 647) and transferrin receptor (*green*, Atto

A DLD-1 GD3S *DES2*^{-/-} genome seq.

WT 5' CAACGCGGCCTTCGGCACGGG 3' -52+1
 5' ----- 3' -52+1
 5' ----- 3' -52+1
DES2^{-/-} 5' ----- GCACGGG 3' -31
 5' ----- GCACGGG 3' -31
 5' ----- GCACGGG 3' -31
 5' ----- GCACGGG 3' -31
 5' ----- GCACGGG 3' -31

DLD-1 GD3S *FA2H*^{-/-} genome seq.

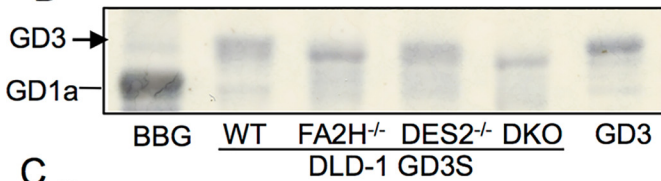
WT 5' CTTTCGTGCGGCACC ACCCGGG 3' -1
 5' CTTTCGTGCGGCACC - CCCGGG 3' -1
 5' CTTTCGTGCGGCACC - CCCGGG 3' -1
 5' CTTTCGTGCGGCACC - CCCGGG 3' -1
 5' CTTTCGTGCGGC - - - - CCCGGG 3' -4
 5' CTTTCGTGCGGC - - - - CCCGGG 3' -4
 5' CTTTCGTGCGGC - - - - CCCGGG 3' -4
 5' CTTTCGTGCGGC - - - - CCCGGG 3' -4

DLD-1 GD3S *DES2*^{-/-}/*FA2H*^{-/-} genome seq.

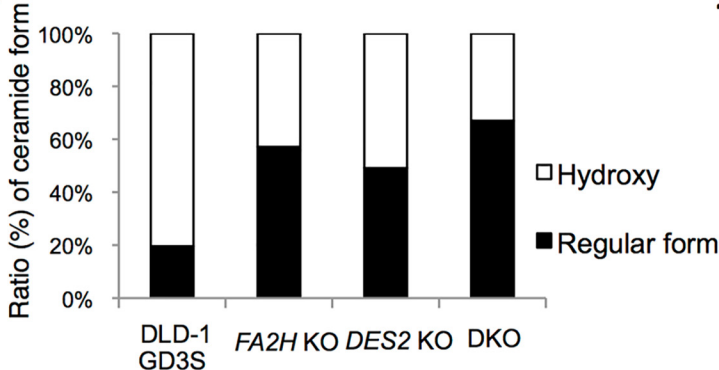
WT 5' CAACGCGGCCTTCGGCACGGG 3' -1
 5' CAACGCGGCCTTCG - CACGGG 3' -1
 5' CAACGCGGCCTTCG - CACGGG 3' -1
 5' CAACGCGGCCTTCG - CACGGG 3' -1
 5' CAACGCGGCCTTCG - CACGGG 3' -1
 5' ----- 3' -56
 5' ----- 3' -56
 5' ----- 3' -56

WT 5' CTTTCGTGCGGCACC ACCCGGG 3' -1
 5' CTTTCGTGCGGCACC - CCCGGG 3' -1
 5' CTTTCGTGCGGCACC - CCCGGG 3' -1
 5' CTTTCGTGCGGCACC - CCCGGG 3' -1
 5' CTTTCGTGCGGC - - - - CCCGGG 3' -4
 5' CTTTCGTGCGGC - - - - CCCGGG 3' -4
 5' CTTTCGTGCGGC - - - - CCCGGG 3' -4
 5' CTTTCGTGCGGC - - - - CCCGGG 3' -4

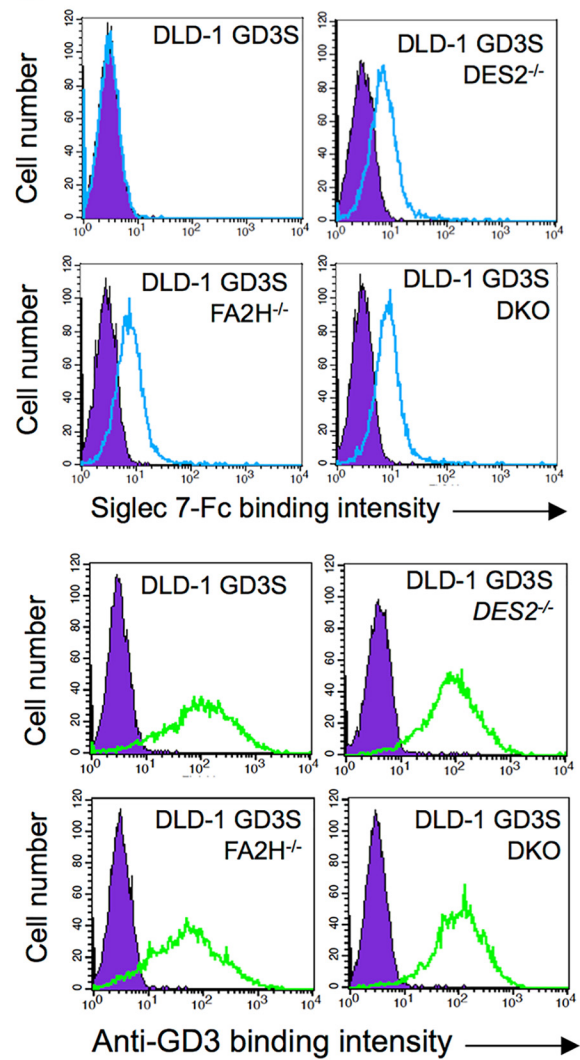
B resorcinol



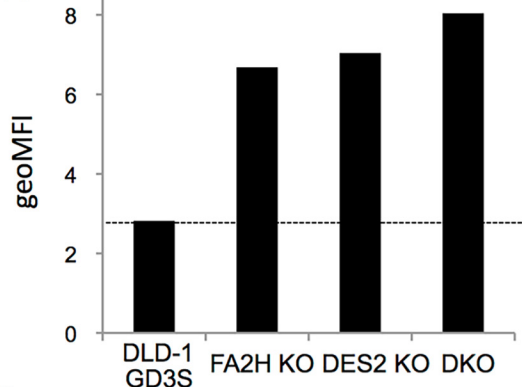
C



D



E



Ceramide structures involved in the recognition of Siglec-7

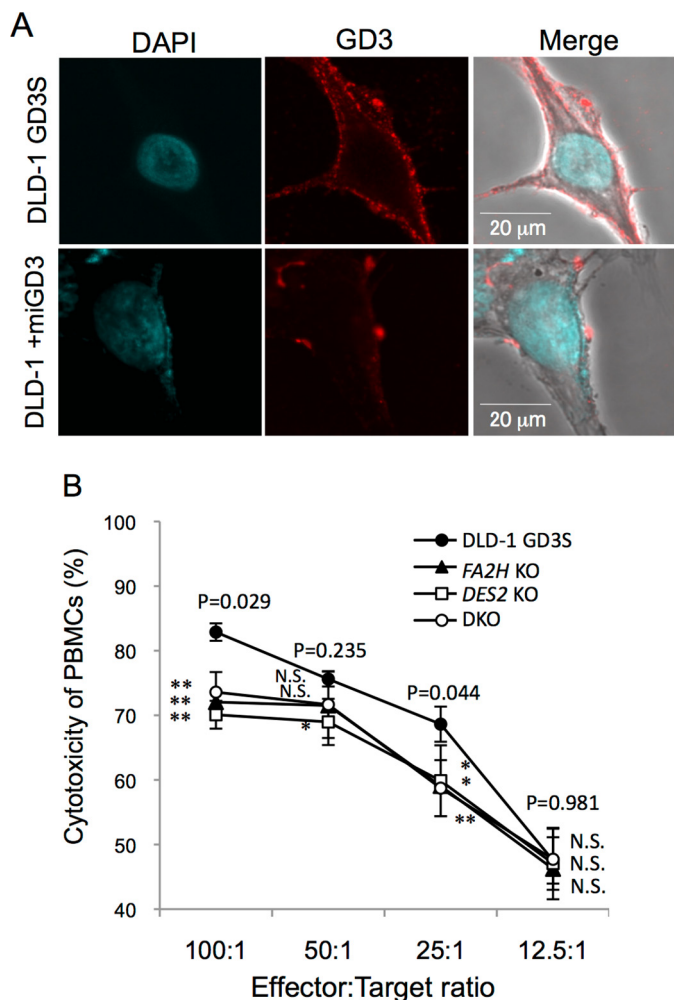


Figure 6. Localization of GD3 and effects of KO of DES2 and/or FA2H on the sensitivity to NK cell killing. A, localization of endogenous and milk-derived GD3. GD3 was stained by mAb R24, and then by an FITC-labeled secondary antibody after fixation with 4% paraformaldehyde in PBS. Confocal images were obtained using FluoviewFV10™ (Olympus). B, cytotoxic activity of human healthy donor-derived PBMCs toward DLD-1 GD3S and various KO cells was measured by LDH release detection kit. LDH-coupled enzymatic product (a red formazan product) was determined by absorbance at 490 nm. The percent cytotoxicity was calculated according to manufacturer's protocol. DAPI, 4,6-diamidino-2-phenylindole.

488, a nonraft marker) (Fig. 8, left panel), DLD-1 GD3S DKO cells showed no white spots at all (Fig. 8, right panel).

All these results indicated the differences in modes of GD3 expression on the cell surface depending on its lipid structures. Supposed mechanisms for differential binding of Siglec-7 to GD3 with phytoceramide and/or 2C hydroxylated FA-containing ceramide are summarized in a schema in Fig. 9.

Discussion

The majority of studies on structures and function of glycosphingolipids has been performed by focusing on the sugar

moiety (16). Glycosphingolipids consist of hydrophilic portions with carbohydrate chains and hydrophobic lipid portions, ceramides. Ceramides can be further divided into fatty acids and LCBs. One of the most intriguing points of glycosphingolipids has been polymorphism in the carbohydrate moieties, and significance of individual sugar structures has been analyzed in various biological processes such as development, differentiation, and malignant transformation of cells (16). Modification of carbohydrates in GD3 by acetylation should also be considered in the analysis of Siglec-7 binding, because O-acetylation of sialic acids has been known to largely affect the binding and their effects (17).

In this study, we have analyzed glycosphingolipid structures recognized by Siglec-7, because Siglec-7 differentially bound ganglioside GD3 from distinct derivations expressed on a colon cancer cell line. In our results, only GD3 with regular form (C4/C5 double bond LCB and nonhydroxylated FA-containing) ceramide structures could be recognized by Siglec-7. Consequently, it was demonstrated that Siglec-7 recognized not only sialyl carbohydrate structures but also ceramide structures linked to the disialyl sugar structures. Intensity in flow cytometry with mAb R24, bands of GD3 in TLC, and results of immunocytochemistry strongly suggested that there was no obvious difference in the amount of GD3 on the cell membrane between endogenously generated GD3 in DLD-1 GD3S and that incorporated from milk-derived gangliosides to DLD-1 cells.

Recently, it was shown that the LPS receptor, TLR4-MD2, recognizes only saturated FA-containing Gb4 as an endogenous ligand (18). There were also reports that differences in the length of fatty acids in ceramides affect the biological function of lactosylceramide, *i.e.* activation of neutrophils (19). However, implication of lipid portion in the recognition of glycosphingolipids by their ligands has been scarcely reported.

As enzymes that hydroxylate ceramides, DES2 and FA2H, have been reported and the possibility that unknown hydroxylation enzymes (2-hydroxylase) also exist have been suggested (20). As shown in this study, gene knockout of either *DES2* or *FA2H* resulted in the reduction of hydroxylated GD3 and subsequent emergence of Siglec-7 binding. Simultaneous knockout of these genes further increased Siglec-7 binding. Furthermore, it was also suggested that newly dehydroxylated ceramide-containing GD3 showed reduced sensitivity to the killing by NK cells in PBMCs via interaction with Siglec-7 and subsequent inhibitory signaling (Fig. 6B). Thus, it can be concluded that ceramide structures in glycosphingolipids are involved in not only binding of Siglec-7 but also in the biological effects triggered by their interactions.

As for C2-hydroxylation of fatty acids, there have been intriguing reports on various biological effects of 2-hydroxyceramide-containing glycolipids, *e.g.* stability of myelination and regulation of apoptosis (21). Furthermore, *FA2H* gene expression data

Figure 5. Effects of knockout of DES2 and FA2H on the structure of GD3 and Siglec-7 binding. A, genome sequences of a total of eight clones each after knockout of *DES2* and/or *FA2H* with CRISPR/Cas9 are shown. Because numbers of deleted bases were not in multiples of three in all clones, these gene products should lose correct protein forms. B, KO cell-derived ganglioside bands were compared in HPTLC. C, extracted acidic glycolipids from DLD-1 GD3S and individual KO cells were separated by HILIC-HPLC system and quantified by MRM analysis. The intensities of ions of major components of GD3 (t18:0-24:1/d18:1-24:0 h) and corresponding regular forms (d18:1-24:0) were measured and calculated as "hydroxyl" and "nonhydroxyl" (regular) species. D, FCM analysis by Siglec-7-Fc (upper panel) and anti-GD3 mAb (lower panel). E, summary of FCM analysis. Geometric mean of fluorescence intensity (*geoMFI*) of Siglec-7 binding was measured and presented. These analyses were repeated at least three times with similar results.

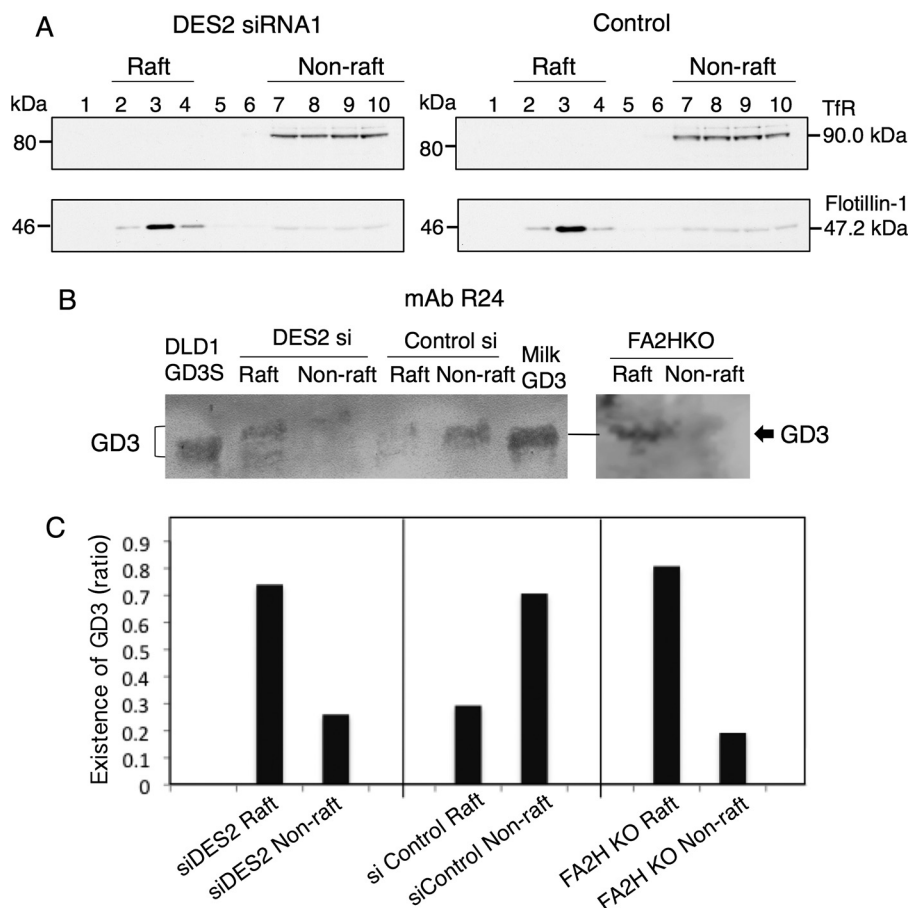


Figure 7. DES2 knockdown and FA2H knockout resulted in recruitment of GD3 to lipid rafts. A, lipid rafts of DLD-1 GD3S transfected with anti-DES2 siRNA twice or DLD-1 GD3S FA2HKO were fractionated by sucrose density gradient ultracentrifugation, and TfR (*non-raft marker*) and Flotillin-1 (*raft marker*) were immunoblotted. B, TLC immunostaining with mAb R24 (anti-GD3) for raft-derived (fractions 2–4) and nonraft-derived (fractions 7–10) gangliosides were performed after pooling and purification with SepPakC18 and DEAE-Sephadex column. Antibody binding was detected using Konica Immunostain HRP-1000 (Konica Minolta) or ECL-Plus (PerkinElmer Life Sciences). C, intensity of the GD3 bands in the individual lanes were quantified using ImageJ software and were presented as % ratios of bands between raft and nonraft in the individual cell lines. Similar results were obtained at least twice, and representative results are shown.

revealed that cancers generally express definitely lower levels of *FA2H* than corresponding normal tissues, *e.g.* skin and colon etc. (GEO entry 79152). Taken together with our results, loss of hydroxylation of ceramides in either LCB or FA in cancers may confer the capability to counter-attack toward the NK cells, leading to escape of cancer cells from immune surveillance system.

A previous study (22) reported that the “intermediate zone,” *i.e.* linkage region between the polar part and the hydrophobic part, was of interest in the physicochemical properties of membranes. It has been long thought that a variation in the number of hydroxyl groups (1–4 hydroxylation) of FA and LCB might be important for the regulation of the potential hydrogen bonds and largely affect membrane stability and barrier properties. Actually, knockdown of *FA2H* leads to enhanced diffusional mobility of raft-associated lipids in the plasma membrane (23). However, co-crystallization of the V-set domain of Siglec-7 with a GT1b analog revealed that Siglec-7 undergoes a large conformational shift upon binding the GT1b analog, leading to suited binding to glycosphingolipid core region (Glc-Cer) of b-series gangliosides (24). *DES2* and *FA2H* are highly expressed in normal colon, whereas the expression levels of them seem to reduce along with increasing degrees of malignancy of tumors.

Whether recognition of sialyl glycosphingolipids by Siglec-7 takes place at single molecular levels or is based on the assembled glycolipids on the cell surface remains to be investigated.

Furthermore, whether hydroxylation of the ceramide portion affects modes of assembly of glycosphingolipids, particularly on the cell surface, is also an intriguing issue. Our results obtained in this study by biochemical analyses (Fig. 7) and also by morphological (imaging) approaches (Fig. S6 and Fig. 8) strongly suggest substantial basis for the differences in Siglec-7 binding depending on the ceramide structures. The binding of Siglec-7 might depend on the intracellular localization of GD3 and probably on the molecular clustering. The discrepancy in the binding of Siglec-7-Fc to GD3 between two situations, *i.e.* on the cell surface of DLD-1 GD3S and on TLC plate (Fig. 1, A and D), might indicate differences in the organization of DLD-1 GD3S-derived GD3 under these two environments.

Experimental procedures

Antibodies and recombinant Siglec-7-Fc

Anti-GD3 mAb R24 (mouse IgG3) was kindly provided by Dr. L. J. Old at Memorial Sloan-Kettering Cancer Center. Anti-

Ceramide structures involved in the recognition of Siglec-7

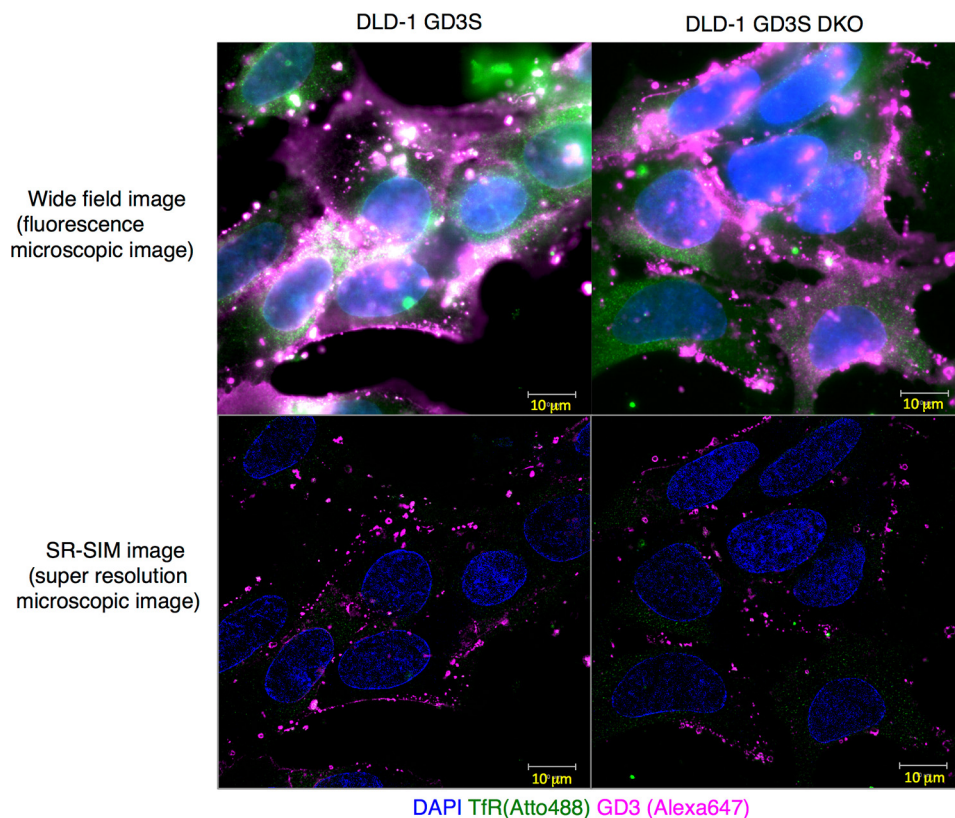


Figure 8. Distribution patterns of GD3 as analyzed by ELYRA super-resolution microscope. Super-resolution imaging of GD3 on DLD-1 GD3S and the DES2/FA2H DKO cells was performed. Cells were seeded on glass coverslips (No. 1^{1/2} high-performance, Zeiss) and fixed with 3% PFA + 0.1% glutaraldehyde PBS. They were reduced with 0.1% NaBH₄ and blocked in 2.5% BSA and 5% normal goat serum. Mouse anti-GD3 mAb R24 and rabbit anti-TfR antibody (H-300, Santa Cruz Biotechnology) were added and incubated for 1 h. Anti-rabbit IgG-ATTO488 (Sigma) and anti-mouse-Alexa 647 (Invitrogen) were added and incubated for 1 h. Washed samples were post-fixed with 3% PFA + 0.1% glutaraldehyde. They were embedded following TDE protocol (27). SR-SIM imaging was performed using LSM880-ELYRA PS.1 system (Zeiss). Wide-field images (*upper panel*) and SR-SIM images (*lower panel*) of DLD-1 GD3S (*left panel*) and DLD-1 GD3S DES2/FA2H DKO (*right panel*) cells are shown. DAPI, 4,6-diamidino-2-phenylindole.

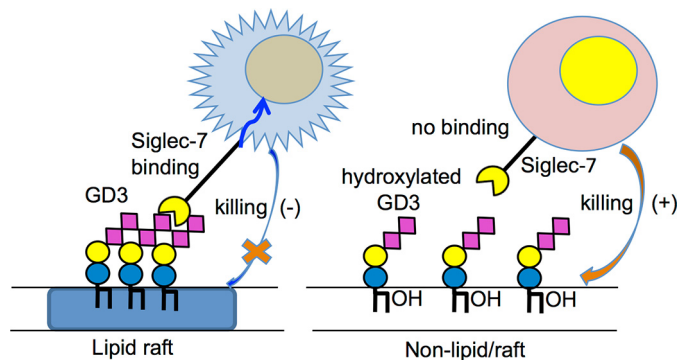


Figure 9. Summary of this study. Hydroxylated ceramide-containing GD3 does not form clusters on the cell surface, leading to nonbinding of Siglec-7, and confers cells with higher sensitivity to NK cell killing. However, regular ceramide-containing GD3 forms clusters in lipid/rafts, leading to binding of Siglec-7, and makes cells less sensitive to NK activity.

GD2 mAb 220-51 (mouse IgG1) was previously generated in our laboratory (4). Anti-mouse IgG conjugated with horseradish peroxidase and anti-mouse IgG conjugated with FITC were from Amersham Biosciences (Little Chalfont, UK). Anti-human IgG Fc-specific antibody conjugated with FITC or phycoerythrin were from BioLegend (Little Chalfont, UK). Siglec-7-Fc is a fusion protein created through the joining of the extracellular domain of Siglec-7 and human IgG1 Fc region. An expression vector pEE14-Siglec-7-Fc was kindly provided by

Dr. Crocker at University of Dundee. Siglec-7-Fc protein was expressed in HEK293T and purified using the protein A-Sepharose™ beads column (GE Healthcare, Little Chalfont, UK).

Cell culture and establishment of ganglioside GD3-expressing cell lines

A human colon adenocarcinoma cell line DLD-1 was maintained in Dulbecco's modified Eagle's medium (DMEM) (NISSUI, Tokyo, Japan) supplemented with 7.5% fetal bovine serum at 37 °C in a humidified atmosphere containing 5% CO₂. GD3S (*ST8SIA1*) cDNA-transfectant DLD-1 GD3S clones were selected in the medium containing 400 μg/ml G418 (Sigma) and maintained in the same condition. These cells were cultured in the G418-deleted medium for ~1 week before being used for some experiments.

FCM

Cell-surface expression of GD3 was analyzed by FCM, FACSCalibur™ (BD Biosciences). Cells were detached by trypsin-EDTA/PBS and incubated with a primary antibody for 45 min on ice and then stained with fluorescein-labeled secondary antibody.

Expression analysis of gangliosides

GD3-expressing DLD-1-transfectant cells were established by GD3 synthase (*ST8SIA1*) cDNA transfection into DLD-1.

For incorporation of exogenous GD3 in DLD-1, bovine milk-derived GD3 was added to DLD-1 culture medium. In brief, DLD-1 (GD3⁻) was cultured in DMEM containing bovine milk GD3 (12.5 μM) for 5 h at 37 °C. After 5 h, the cells were analyzed with FCM to check GD3 expression levels and binding of Siglec-7-Fc.

Isolation of gangliosides and TLC

To prepare total gangliosides from cultured cells, total lipids were extracted by chloroform (C)/methanol (M) 2:1 (v/v) overnight, and at 1:1 (v/v) for 1 h and at 1:2 for 1 h. Resulting extracts were desalted by Sep-Pak C18TM (Waters) and applied to a DEAE-Sephadex A-50TM (GE Healthcare, Little Chalfont, UK). They were separated into neutral fraction (flow-through) and acidic fraction (elution with C/M, 0.8 M sodium acetate, 30:60:8). The acidic fractions were analyzed by HPTLC Silica Gel 60TM (Merck Millipore, Darmstadt, Germany) after desalting and resorcinol spray. TLC immunostaining and mass spectrometry (MS) were performed for structural analysis. TLC and TLC immunostaining were done as reported previously (25).

Isolation of gangliosides from bovine milk

Highly-concentrated ganglioside powder by trypsin digestion of milk and subsequent gel filtration was used for extraction with C/M (1:1). The extracts were applied for ion-exchange column (DEAE-Toyoppearl acetate form), and gangliosides were eluted by 0.5 M sodium acetate in MeOH. After desalting and concentration, samples were applied for silica gel column, and gangliosides were eluted by C/M (2:8) and concentrated by evaporation. More than 90% was gangliosides in TLC-resorcinol.

MS

TLC-developed samples were analyzed directly using ESI robotic ion source TriVersa NanoMate LESATM system and QTRAP 6500TM (ABSciex, MA). Glycolipids extracted from DLD-1 GD3S were separated on an aluminum sheet-backed HPTLC Silica Gel 60TM (Merck Millipore, Darmstadt, Germany) using a solvent system as described above. The plate was stained by primuline solution (0.001% of acetone/water, 80:20), and the location of GD3 was decided. Then, glycolipids were blotted onto a polyvinylidene difluoride membrane with TLC Thermal BlotterTM (ATTO Corp., Tokyo, Japan). GD3 on the pre-programmed position was automatically extracted by the robot with a special tip containing 10 μl of extraction solvent (C/M = 2:1, 5 mM ammonium formate) and then induced into ion source. The precursor ion scan of 290 m/z ([Neu5Ac-H]⁻) in negative ion mode was performed for screening of GD3 molecular species.

For structural analysis, enhanced product ion scan against m/z was performed by a trap fill time of 1 ms in positive and negative modes. MRM analysis for quantification of several ceramide molecular species of GD3 was performed using QTRAP6500 system combined with Shimadzu ProminenceTM HPLC system (Shimadzu, Kyoto, Japan). Samples were injected into the HPLC equipped with a HILIC column (BEH amide, Waters). LC separation was performed with linear gradient (0–5 min, 0% B; 5–30 min, 0–100% B; equilibration, 10 min, 0% B) of solvent A (83% acetonitrile and 17% water with 1 mM

ammonium formate) and solvent B (50% acetonitrile and 50% water with 50 mM ammonium formate) at an estimated flow rate of 150 $\mu\text{l}/\text{min}$ and column temperature was set at 40 °C. For LESA and MRM analysis, ion spray voltage, declustering potential, and collision-induced dissociation conditions were –4500, –120, and –40 V in negative ion mode and 5500, 45, and 45 V in positive ion mode.

Knockout of DES2 and FA2H with CRISPR/Cas9 system

The pX330-sgRNA-Cas9 plasmid was kindly provided by Dr. M. Ikawa at Osaka University. For preparing knockout cells of *DES2* and *FA2H* genes using the CRISPR/Cas9 system, we designed sgRNA against individual genes according to previous reports (26). Their CRISPR/Cas9 target genome sequences are 5'-GCACAACGCGGCCCTTCGGCACGG-3' on exon 2 of human *DES2* and 5'-AGCTTCGTGCGGCACCACCCGGG-3' on exon 1 of human *FA2H*. The 5'-NGG-3' is a protospacer adjacent motif sequence. Oligonucleotides for the knockout system of CRISPR/Cas9 expression vector pX330-sgRNA are forward primer 5'-caccgcacaacgcggccttcggca-3' and reverse primer 5'-aaactgccgaaggccggtgtgca-3' for pX330-sgRNA *hDES2*, and forward primer 5'-caccgagcttcgtgcccaccacccc-3' and reverse primer 5'-aacgggtggtgcccgcacgaagctc-3' for pX330-sgRNA *hFA2H*.

Synthesized oligonucleotides corresponding to parts of individual genes adding a restriction enzyme BbsI sequence were inserted into pX330-Cas9 plasmid after BbsI treatment. These vectors were amplified in Stbl3-competent cells (Invitrogen). For establishment of *DES2* and *FA2H* KO cell lines, these sgRNAs and Cas9 expression vectors together with blasticidin S-resistance gene and EGFP expression vector were co-transfected into DLD-1 GD3S cell. Then, these cells underwent selection in the presence of blasticidin S (at 8 $\mu\text{g}/\text{ml}$) (Funakoshi, Tokyo, Japan) and were checked that EGFP is negative, indicating no stable expression of sgRNA and Cas9. After establishment of transfectant clones by limiting dilution, genome sequences of *DES2* and *FA2H* were checked. In brief, their target genomic DNA was amplified using KOD FXTM (TOYOBO), and 3'-adenine was added by GoTaq polymeraseTM (Promega, WI). Then, the products were cloned by TOPO TATM cloning kit (Invitrogen) and sequenced by BigDyeTM terminator version 1.1 cycle sequence kit (Applied Biosystems) using the M13 forward primers. The BigDye products were applied for PRISM 3100 Genetic AnalyzerTM (Applied Biosystems). Their sequences of at least eight clones for each transfectant were analyzed.

Immunocyto staining of GD3

Cells were plated on a round cover glass in wells of 24-well plates and incubated overnight in DMEM supplemented with 7.5% fetal calf serum at 37 °C. The next day, after washing three times with plain DMEM, milk-derived GD3 in plain DMEM was added (12.5 μM) and incubated for 7 h at 37 °C. Cells were fixed with paraformaldehyde (4% in PBS) for 10 min at room temperature and then washed twice with PBS. Nonspecific binding was blocked with BSA (5% in PBS) for 1 h at room temperature. Cells were incubated with mAb R24 (1:200) in PBS containing 2% BSA for 1 h at room temperature. After

Ceramide structures involved in the recognition of Siglec-7

being washed with PBS, cells were incubated with Alexa 568-conjugated goat anti-mouse-IgG (1:200) (Invitrogen) in PBS containing 2% BSA for 1 h at room temperature. After washing twice with PBS, cells were imaged using a confocal microscope (Fluoview FV10TM, Olympus, Tokyo, Japan).

Cytotoxicity assay with PBMCs

PBMCs were obtained by Ficoll-PaqueTM (GE Healthcare, Little Chalfont, UK) from healthy donors' peripheral blood. The cytotoxicity of NK cells (PBMCs) against Siglec-7-Fc-reactive or nonreactive DLD-1 GD3S was assessed using CytoTox 96 Nonradioactive Cytotoxicity AssayTM kit (Promega, WI) according to the manufacturer's instruction. E/T indicates ratio of effector (PBMCs) to target (DLD-1 GD3S and knockout cells). Human cells were used in accordance with the Ethics Committee of Nagoya University Graduate School of Medicine following the Declaration of Helsinki principles.

Separation of raft/nonraft fractions

Lipid rafts of DLD-1 GD3S cells and those treated with anti-DES2 siRNA or DLD-1 GD3S FA2H KO were fractionated by sucrose density gradient ultracentrifugation, and TfR (nonraft marker) and flotillin-1 (raft marker) were immunoblotted as described previously (8).

TLC immunostaining

Gangliosides were collected from raft fractions (fractions 2–4) and nonraft fractions (fractions 7–10) from ultracentrifugation of Triton X-100 extracts. They were pooled and purified with SepPak C18 and DEAE-Sephadex column. Gangliosides were separated and heat-blotted as described in "MS". Then, the membrane was immunoblotted using anti-GD3 mAb R24, and antibody binding was detected using Konica Immunostain HRP-1000 (Konica Minolta) or ECL-Plus (PerkinElmer Life Sciences).

Super-resolution imaging

Cells were seeded on glass coverslips (No. 1^{1/2} high-performance, Zeiss) and fixed with 3% PFA + 0.1% glutaraldehyde PBS for 10 min at room temperature. They were reduced with 0.1% NaBH₄ for 7 min and blocked in 2.5% BSA and 5% normal goat serum. mAb R24 and rabbit anti-TfR antibody (H-300, Santa Cruz Biotechnology) were added and incubated for 1 h at room temperature. Anti-rabbit IgG-ATTO488 (Sigma) and anti-mouse-Alexa 647 (Invitrogen) were added and incubated for 1 h at room temperature. Washed samples were post-fixed with 3% PFA + 0.1% glutaraldehyde. They were embedded by 2,2'-thiodirithanol (TDE) protocol (27). Super-resolution structured illumination microscopy (SR-SIM) imaging was performed with LSM880-ELYRA PS.1 system (Zeiss).

Statistics

One-way analysis of variance was performed to compare means of the percent cytotoxicity of PBMCs toward Siglec-7-Fc-nonreactive clone (DLD-1 GD3S) and three Siglec-7-Fc-reactive clones (FA2H KO, DES2 KO, and DKO) by statistics software StatPlus:mac LE version 6.1.60 (AnalystSoft, CA).

Student's *t* test was performed by Excel 2011 for mac (Microsoft, WA).

Author contributions—N. H., S. I., A. T., T. O., A. Y., and Koichi Furukawa conceptualization; N. H., S. I., A. T., Keiko Furukawa, Y. O., and Koichi Furukawa data curation; N. H. software; N. H. formal analysis; N. H. and Koichi Furukawa funding acquisition; N. H., S. I., A. T., Keiko Furukawa, Y. O., and Koichi Furukawa validation; N. H., S. I., A. T., and R. H. B. investigation; N. H., S. I., A. T., R. H. B., and Koichi Furukawa visualization; N. H., S. I., A. T., R. H. B., Keiko Furukawa, Y. O., and Koichi Furukawa methodology; N. H. writing-original draft; T. O., A. Y., Keiko Furukawa, Y. O., and Koichi Furukawa supervision; T. O., A. Y., and Koichi Furukawa project administration; Koichi Furukawa resources; Koichi Furukawa writing-review and editing.

Acknowledgments—We thank P. R. Crocker at Dundee University for providing an expression vector pEE14-Siglec-7-Fc, and M. Ikawa at Osaka University for providing plasmids for CRISPR/Cas9 system. We also thank T. Mizuno, Y. Nakayasu, Y. Kitaura, and S. Yamamoto for technical assistance. Mass spectrometry was performed at the Division for Medical Research Engineering, Nagoya University Graduate School of Medicine.

References

1. Hakomori, S. (1984) Tumor-associated carbohydrate antigens. *Annu. Rev. Immunol.* **2**, 103–126 [CrossRef Medline](#)
2. Peracaula, R., Barrabés, S., Sarrats, A., Rudd, P. M., and de Llorens, R. (2008) Altered glycosylation in tumours focused to cancer diagnosis. *Dis. Markers* **25**, 207–218 [CrossRef Medline](#)
3. Furukawa, K., Hamamura, K., Ohkawa, Y., Ohmi, Y., and Furukawa, K. (2012) Disialyl gangliosides enhance tumor phenotypes with differential modalities. *Glycoconj. J.* **29**, 579–584 [CrossRef Medline](#)
4. Yoshida, S., Fukumoto, S., Kawaguchi, H., Sato, S., Ueda, R., and Furukawa, K. (2001) Ganglioside G(D2) in small cell lung cancer cell lines: enhancement of cell proliferation and mediation of apoptosis. *Cancer Res.* **61**, 4244–4252 [Medline](#)
5. Hamamura, K., Furukawa, K., Hayashi, T., Hattori, T., Nakano, J., Nakashima, H., Okuda, T., Mizutani, H., Hattori, H., Ueda, M., Urano, T., Lloyd, K. O., and Furukawa, K. (2005) Ganglioside GD3 promotes cell growth and invasion through p130Cas and paxillin in malignant melanoma cells. *Proc. Natl. Acad. Sci. U.S.A.* **102**, 11041–11046 [CrossRef Medline](#)
6. Cazet, A., Bobowski, M., Rombouts, Y., Lefebvre, J., Steenackers, A., Popa, I., Guérardel, Y., Le Bourhis, X., Tulasne, D., and Delannoy, P. (2012) The ganglioside G(D2) induces the constitutive activation of c-Met in MDA-MB-231 breast cancer cells expressing the G(D3) synthase. *Glycobiology* **22**, 806–816 [CrossRef Medline](#)
7. Yeh, S. C., Wang, P. Y., Lou, Y. W., Khoo, K. H., Hsiao, M., Hsu, T. L., and Wong, C. H. (2016) Glycolipid GD3 and GD3 synthase are key drivers for glioblastoma stem cells and tumorigenicity. *Proc. Natl. Acad. Sci. U.S.A.* **113**, 5592–5597 [CrossRef Medline](#)
8. Ohkawa, Y., Momota, H., Kato, A., Hashimoto, N., Tsuda, Y., Kotani, N., Honke, K., Suzumura, A., Furukawa, K., Ohmi, Y., Natsume, A., Wakabayashi, T., and Furukawa, K. (2015) Ganglioside GD3 enhances invasiveness of gliomas by forming a complex with platelet-derived growth factor receptor α and Yes kinase. *J. Biol. Chem.* **290**, 16043–16058 [CrossRef Medline](#)
9. Kaneko, K., Ohkawa, Y., Hashimoto, N., Ohmi, Y., Kotani, N., Honke, K., Ogawa, M., Okajima, T., Furukawa, K., and Furukawa, K. (2016) Neogenin, defined as a GD3-associated molecule by enzyme-mediated activation of radical sources, confers malignant properties via intracytoplasmic domain in melanoma cells. *J. Biol. Chem.* **291**, 16630–16643 [CrossRef Medline](#)

10. Heyningen, S., Van. (1974) Cholera toxin: interaction of subunits with ganglioside GM1. *Science* **183**, 656–657 [CrossRef Medline](#)
11. Crocker, P. R., Kelm, S., Hartnell, A., Freeman, S., Nath, D., Vinson, M., and Mucklow, S. (1996) Sialoadhesin and related cellular recognition molecules of the immunoglobulin superfamily. *Biochem. Soc. Trans.* **24**, 150–156 [CrossRef Medline](#)
12. O'Reilly, M. K., and Paulson, J. C. (2010) Multivalent ligands for siglecs. *Methods Enzymol.* **478**, 343–363 [CrossRef Medline](#)
13. Miyazaki, K., Ohmori, K., Izawa, M., Koike, T., Kumamoto, K., Furukawa, K., Ando, T., Kiso, M., Yamaji, T., Hashimoto, Y., Suzuki, A., Yoshida, A., Takeuchi, M., and Kannagi, R. (2004) Loss of disialyl Lewis(a), the ligand for lymphocyte inhibitory receptor sialic acid-binding immunoglobulin-like lectin-7 (Siglec-7) associated with increased sialyl Lewis(a) expression on human colon cancers. *Cancer Res.* **64**, 4498–4505 [CrossRef Medline](#)
14. Kawasaki, Y., Ito, A., Kakoi, N., Shimada, S., Itoh, J., Mitsuzuka, K., and Arai, Y. (2015) Ganglioside, disialosyl globopentaosylceramide (DSGb5), enhances the migration of renal cell carcinoma cells. *Tohoku J. Exp. Med.* **236**, 1–7 [CrossRef Medline](#)
15. Nicoll, G., Avril, T., Lock, K., Furukawa, K., Bovin, N., and Crocker, P. R. (2003) Ganglioside GD3 expression on target cells can modulate NK cell cytotoxicity via siglec-7-dependent and -independent mechanisms. *Eur. J. Immunol.* **33**, 1642–1648 [CrossRef Medline](#)
16. Regina Todeschini, A., and Hakomori, S. I. (2008) Functional role of glycosphingolipids and gangliosides in control of cell adhesion, motility, and growth, through glycosynaptic microdomains. *Biochim. Biophys. Acta* **1780**, 421–433 [CrossRef Medline](#)
17. Schauer, R. (2009) Sialic acids as regulators of molecular and cellular interactions. *Curr. Opin. Struct. Biol.* **19**, 507–514 [CrossRef Medline](#)
18. Kondo, Y., Ikeda, K., Tokuda, N., Nishitani, C., Ohto, U., Akashi-Takamura, S., Ito, Y., Uchikawa, M., Kuroki, Y., Taguchi, R., Miyake, K., Zhang, Q., Furukawa, K., and Furukawa, K. (2013) TLR4–MD-2 complex is negatively regulated by an endogenous ligand, globotetraosylceramide. *Proc. Natl. Acad. Sci. U.S.A.* **110**, 4714–4719 [CrossRef Medline](#)
19. Iwabuchi, K., Prinetti, A., Sonnino, S., Mauri, L., Kobayashi, T., Ishii, K., Kaga, N., Murayama, K., Kurihara, H., Nakayama, H., Yoshizaki, F., Takamori, K., Ogawa, H., and Nagaoka, I. (2008) Involvement of very long fatty acid-containing lactosylceramide in lactosylceramide-mediated superoxide generation and migration in neutrophils. *Glycoconj. J.* **25**, 357–374 [CrossRef Medline](#)
20. Dan, P., Edvardson, S., Bielawski, J., Hama, H., and Saada, A. (2011) 2-Hydroxylated sphingomyelin profiles in cells from patients with mutated fatty acid 2-hydroxylase. *Lipids Health Dis.* **10**, 84 [CrossRef Medline](#)
21. Kota, V., and Hama, H. (2014) 2'-Hydroxy ceramide in membrane homeostasis and cell signaling. *Adv. Biol. Regul.* **54**, 223–230 [CrossRef Medline](#)
22. Karlsson, K. A. (1998) On the character and functions of sphingolipids. *Acta Biochim. Pol.* **45**, 429–438 [Medline](#)
23. Guo, L., Zhou, D., Pryse, K. M., Okunade, A. L., and Su, X. (2010) Fatty acid 2-hydroxylase mediates diffusional mobility of raft-associated lipids, GLUT4 level, and lipogenesis in 3T3-L1 adipocytes. *J. Biol. Chem.* **285**, 25438–25447 [CrossRef Medline](#)
24. Attrill, H., Imamura, A., Sharma, R. S., Kiso, M., Crocker, P. R., and van Aalten, D. M. (2006) Siglec-7 undergoes a major conformational change when complexed with the alpha(2,8)-disialyl-ganglioside GT1b. *J. Biol. Chem.* **281**, 32774–32783 [CrossRef Medline](#)
25. Furukawa, K., Aixinjueluo, W., Kasama, T., Ohkawa, Y., Yoshihara, M., Ohmi, Y., Tajima, O., Suzumura, A., Kittaka, D., and Furukawa, K. (2008) Disruption of GM2/GD2 synthase gene resulted in overt expression of 9-O-acetyl GD3 irrespective of Tis21. *J. Neurochem.* **105**, 1057–1066 [CrossRef Medline](#)
26. Mashiko, D., Fujihara, Y., Satouh, Y., Miyata, H., Isotani, A., and Ikawa, M. (2013) Generation of mutant mice by pronuclear injection of circular plasmid expressing Cas9 and single guided RNA. *Sci. Rep.* **3**, 3355 [CrossRef Medline](#)
27. Mito, M., Kawaguchi, T., Hirose, T., and Nakagawa, S. (2016) Simultaneous multicolor detection of RNA and proteins using super-resolution microscopy. *Methods* **98**, 158–165 [CrossRef Medline](#)